AAS 93-570

THE ROLE OF ANOMALOUS SATELLITE-FIXED ACCELERATIONS IN TOPEX/POSEIDON ORBIT MAINTENANCE*

R. B. Frauenholz,† T. W. Hamilton,‡ B. E. Shapiro,†† and R. S. Bhat‡‡
Jet Propulsion Laboratory, California Institute of Technology, Pasadena, Ca.

Shortly after the launch of TOPEX/Poseidon on 10 August 1992 orbit determination indicated orbital decay levels -60 times larger than could be explained by atmospheric drag. Outgassing, a complex process of molecular releases from satellite non-metallic parts, was the most likely source of these early decay rates. The high decay levels steadily declined during the first six weeks while a planned sequence of six orbit adjust maneuvers placed the satellite in the operational orbit to precisely overfly a predetermined repeat ground track. At the same time, on-going orbit trend analysis revealed the presence of residual along-track forces comparable to atmospheric drag which clearly exhibited a body-fixed origin. These anomalous forces cause either orbital decay or boost, depending on the satellite attitude and solar array articulation mode. As such, these along-track forces can either add to, or oppose, the resident orbital decay due to drag.

Orbit maintenance maneuver design was expected to depend primarily on effective predictions of atmospheric drag, but now also depends equally on a reliable predictions of the anomalous along-track forces. The basic behavior of the anomalous forces has been established, evolving from quite unknown character early in the mission to reasonably predictable by mid-August 1993. This paper describes the method used to estimate the anomalous forces and presents an empirical prediction model for each of the four satellite yaw control modes, also reflecting the significant influences of a newly-adopted operational strategy to bias solar array pointing for battery lifetime enhancement.

INTRODUCTION

TOPEX/Poseidon was successfully launched by an Ariane 42P from French Guiana on 10 August 1992. The primary goals of this joint US/French mission are to study ocean circulation and its interaction with the atmosphere, to better understand climate change; to improve knowledge of heat transport in the ocean; to model ocean tides; and to study the marine gravity field. To accomplish these objectives requires determination of ocean surface height to an accuracy of 13 cm utilizing a combination of satellite altimetry and precision orbit determination[1] based primarily on laser ranging measurements. These objectives are to be accomplished over a primary mission lifetime of three years, with a possible two-year extension.

* The research described in this paper was carried out by the Jet Propulsion Laboratory, California Institute of Technology, under contract with the National Aeronautics and Space Administration.

† Technical Manager, Member AIAA
‡ Senior Technical Manager, Associate Fellow AIAA
†† Member Technical Staff, Member AAS, Member AIAA
‡‡ Member Technical Staff

The Jet Propulsion Laboratory (JPL) is responsible for TOP1;X/Poseidon mission operations, including operational navigation. Major navigation functions include all maneuver design, evaluation, and related orbit analysis. Operational orbit determination support is provided to JPI. by the Flight Dynamics Facility at the Goddard Space Flight Center (GSFC/FDF) using tracking data acquired via the NASA Tracking and Data Relay Satellite System (TDRSS). Detailed interfaces and procedures for exchanging maneuver and orbit determination data between JPL and the GSFC/FDF were established and thoroughly tested prior to launch to assure all perform ancc requirements were satisfied.[2]

ORBIT M AI NTENANCE REQUIREMENTS

A planned sequence of six orbit adjust maneuvers[3] began soon after launch to precisely place the satellite in a near-circular frozen orbit at an inclination of -66" and an equatorial altitude of -1336 km. During the maneuvering process, the orbit ground track was precisely aligned with a reference ground track which repeats every 127 revolutions over -9.9 days, while also overflying single US and French altimeter verification sites. 't"his sequence was completed on 21 September 1992,42 days after launch.[4]

Maneuvers arc periodically required to maintain the operational orbit and attendant ground track, The specified control and maneuver scheduling constraints require that:

1) 95% of all equatorial crossings arc contained within a 2-km longitude band at each orbit node,

2) 95% of all altimeter verification site overflights arc within ±1 km during the initial verification phase (at least first six months),

3) maneuver spacings arc at least 30 days, time-phased to occur near the boundary of pre-determined 9.9-day ground track repeat cycles to limit interference with precision orbit determination, and

4) the bum occurs over land to preclude interruption of ocean altimetry.

Maneuver design also reflects satellite health and safety concerns by satisfying telecommunications, thermal, and power constraints when selecting tbc maneuver location near the cycle boundaries.

SATELLITE YAW CONTROL MODES AND SOLAR ARRAY POINTING STRATEGY

YAW' CONTROL MODES

TOPEX/Poseidon is a three-axis stabilized satellite (Figure 1) with the altimeter boresight always pointed normal to the reference ellipsoid. At the same time, near-continuous sinusoidal yaw steering about the local nadir and solar array (SA) pitching combine to maintain the SA pointed near the sun for power optimization. The yaw steering strategy is used continuously except when $-15° < \beta' < 15°$, where β' is the angle between the orbit plane and the sunline (e.g., Figures 2c and 11). When β' is near these angular limits a fixed yaw attitude is utilized to avoid excessive yaw rates. The satellite is positioned at a zero yaw angle ($\psi_s = 0°$) when $0° < \beta' < 15°$ (flying forward), whereas $\psi_s = 180°$ is utilized when $-15° < \beta' < 0°$ (flying backward). Accordingly, a yaw flip maneuver is required near $\beta' = 0°$ to keep the SA on the sunlight side of the satellite. The β' angle passes through zero once every -56 days as the satellite orbit node regresses ~2.2°/day and the earth moves in its orbit -1 °/day.

The sinusoidal yaw steering algorithm is described in Eq. (1), where $\Omega = 90° + v - \nu_{Sun}$, ν_{Sun} is the angle of the projection of the earth-sun line into the orbit plane measured from perigee, and v is the true anomaly of the satellite. Solar noon is defined by $\Omega = 90°$.

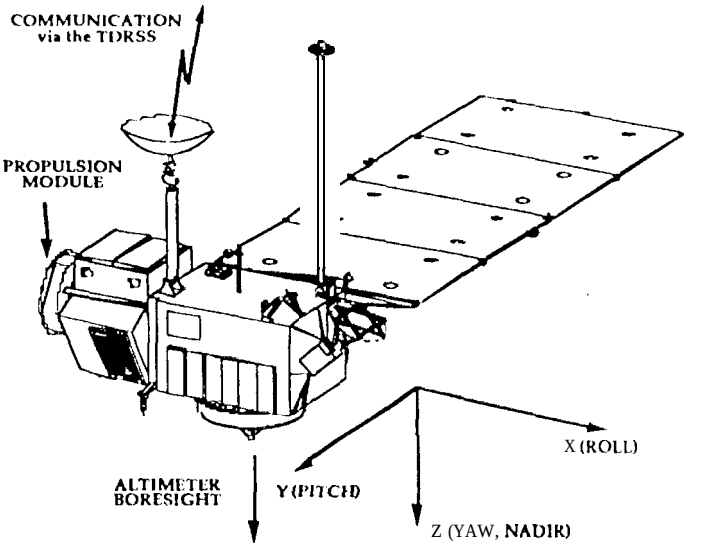

Figure 1 TOPEX/Poseidon Satellite

$$
\begin{aligned}
/? \text{ '215":} \quad & \psi_S = 90^\circ + (90^\circ - \beta')\cos\Omega && \text{(positive yaw steering)} \\
O<p'<is": \quad & \psi_S = 0^\circ && \text{(flying forward)} \\
-15"</? '<0: \quad & \psi_S = 180^\circ && \text{(flying backward)} \\
\beta' \le -15^\circ: \quad & \psi_S = -90^\circ - (90^\circ - \beta')\cos\Omega && \text{(negative yaw steering)}
\end{aligned} \tag{1}
$$

SOLAR ARRAY POINTING STRATEGY

In each yaw mode, the original plan was to continuously pitch the solar array so that it was as nearly normal to the sun as possible. This strategy required that the solar array pitch angle, γ, be set to γ_{opt}, where

$$\gamma_{opt} = 180^\circ - \tan^{-1}\left[\frac{\sin\Omega\cos\beta'}{\cos\psi_S\cos\Omega\cos\beta' - \sin\psi_S\sin\beta'}\right] \tag{2}$$

When the SA ccl] side normal parallels the satellite +X direction, $\gamma \equiv O$. Provision was made to bias the solar array from its optimal direction by an angle B. In each yaw mode the solar array pitch angle is controlled to $\gamma_{opt} + B$, where B > O" is referred to as a *feuding bias*. The resulting pitch angle as a function of orbit angle Ω and yaw control mode is given by Eq. (3).

$$
\begin{aligned}
\gamma &= 180^\circ + B - \Omega && \text{for } \psi_s = 180" \text{ (fixed yaw, fly backward)} \\
\gamma &= \Omega + B && \text{for } \psi_s = 0^\circ \text{ (fixed yaw, fly forward)} \\
\gamma &\approx 180^\circ + B - (90^\circ + \beta')\sin\Omega && \text{(negative yaw steering, } \beta' < -15^\circ) \\
\gamma &\approx 180^\circ - 1\text{-}13 - (90^\circ - \beta')\sin\Omega && \text{(positive yaw steering, } \beta' > 15^\circ)
\end{aligned} \tag{3}
$$

The equations for yaw steering arc approximate and arc shown only to characterize the *windshield wiper* motion of the array in those control modes.

Shortly before launch, a plan was adopted to usc the pitch bias *B* to limit the peak battery charging currents to 20 Amperes. Initially a -r-55" value was employed on 28 Aug 92; it was

refined to 57.5" on 12 Sep 92. More recently, on 27 July 1993, the bias was reduced to 53' to compensate for declining solar array output.

While this strategy seems to be lengthening the battery lifetime, it introduces forces normal to the sunline that are not included in the radiation pressure models adopted for joint use by JPL and the GSFC/FDF. These unmodeled forces introduce errors affecting the ground track that depend on the yaw control mode. Undemanding and effectively modeling these effects are an important part of the orbit maintenance process and a major focus of this paper.

INITIAL MEASURES OF AN ANOMALOUS FORCE

Pre-launch studies[6] established atmospheric drag as the major non-gravitational perturbation affecting the satellite ground track, even though the orbital altitude is relatively high at -1336 km. This sensitivity to drag is a consequence of the stringent ±1-km ground track control requirement. Atmospheric drag causes decay in the orbit semi-major axis, resulting in an eastward drift of the satellite ground track that will eventually travel outside the established control boundary. Periodic maneuvers maintain the ground track inside the control boundaries by removing the accumulated orbital decay with an increase in semi-major axis. * The frequency of maneuvers depends on both the drag level and on the accuracy of drag predictions. Effective drag predictions require long-term predictions of atmospheric density derived from predictions of solar and geomagnetic activity.[7] The Jacchia-Roberts atmospheric density model[8,9] effectively accounts for daily variations in solar and geomagnetic activity, although none of the currently available density models reflect flight data at the TOP13X/Poseidon altitude. A faithful representation of the satellite variable mean area (VMA)[6] is also needed. The VMA defines the orbital-average area as a function of β' based on a detailed projected area model developed by Fairchild Space. [10]

To develop an initial trend in the observed orbital decay behavior, the GSFC/FDF first estimated daily drag acceleration multipliers using tracking data acquired via the TDRSS. The daily drag multiplier is $(1+\rho_1)$, where $\rho_1 \simeq 0$ indicates nominal drag. All unmodeled along-track accelerations are then arbitrarily absorbed as drag without necessarily declaring that these effects are actually due to drag. Figure 2(a) shows the trend in daily $(1+\rho_1)$ estimates from launch through the end of 1992, indicating an exponential decline from an initial post-launch value of ~60 times nominal drag to near-nominal levels by late Sep 92 when operational orbit conditions were finally achieved. Figure 2(b) shows the corresponding rate of change in semi-major axis (Eq. 4)[11,12] varied between -200 and +25 cm/day, equivalent to along-track acceleration levels of -1.2 to 8.3 nanometers/sec^2 (or forces between ~3 and 20 μN).

$$\left(\frac{da}{dt}\right)_{drag} = -\frac{(1+\rho_1)\rho A C_D \sqrt{\mu a}}{m}\left[1-\frac{\omega_e \cos i}{n}\right]^2 \qquad (4)$$

where $(1+\rho_1)$ is the drag scale factor ($\rho_1 = 0$ indicates nominal drag), ρ is the average daily atmospheric density, A is the average per orbit reference drag area variation with β'(VMA), C_D is the satellite drag coefficient, μ is the earth gravitational constant, a is the orbit mean semi-major axis, ω_e is the earth rotation rate, i is the orbit inclination, and n is the orbit mean motion.

Normal outgassing is the most likely explanation for the initially high orbital decay rates. The accelerations associated with outgassing arise from imbalances between gas losses through different sides of the satellite. A differential loss of 0.4 grams, at 500 m/s velocity, will produce a force of 2.4 μN, resulting in a 1 nm/s^2 acceleration. If aligned against the velocity vector, this force would cause -18.5 cm/day decay in the mean semi-major axis. An equal force could be generated by only five puffs *per day* from a typical aerosol inhaler.

* Typical maneuver ΔV magnitudes are ≈5 mm/s, raising the semi-major axis by ≈10 meters.

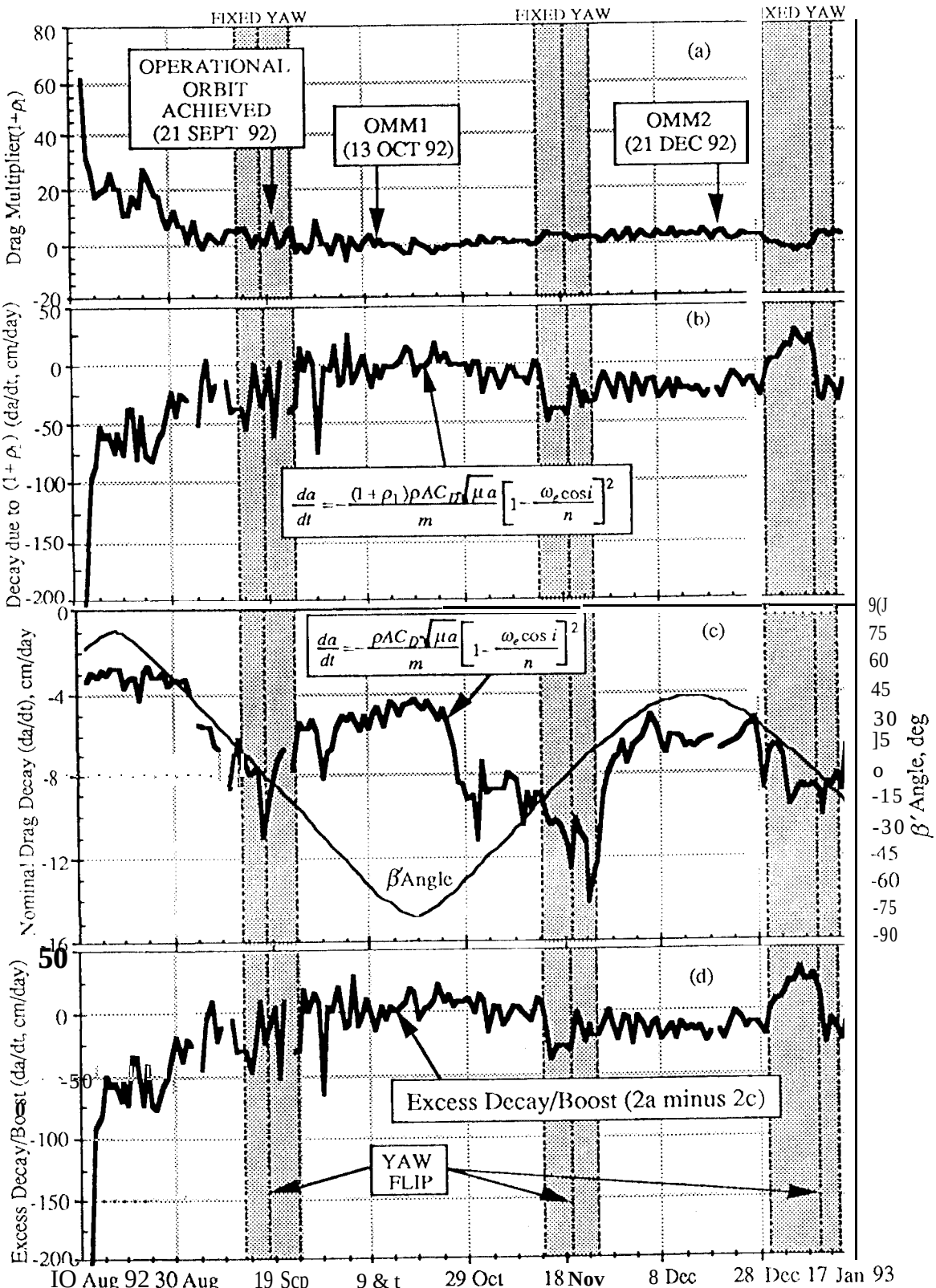

Figure 2(a) Atmospheric Drag Multiplier, (b) Equivalent Total Orbital Decay/host, (c) Orbital Decay Due to Observed Solar Activity, and (d) Excess Decay/Boost Rates.

The orbital decay rates due to drag, estimated by Eq. (4) with $\rho_1 = O$, vary between ~3 and -14 cm/day (Figure 2c). These decay rates are much lower than those implied by the $(1+\rho_1)$ estimates, even after Scp 92 when most of the suspected outgassing had subsided. The distinct lrmg-term systematic signature is duc to the VMA variation with β', whereas the more frequent variations arc caused by changes in the average daily atmospheric density with observed solar activity.

Estimates of orbital decay (or boost) rates in excess of nominal drag (Figure 2d) were obtained by removing the drag decay rates in Figure 2(c) from the total decay/boost rates in Figure 2(b). Figure 2(d) clearly shows excess *boost* rates during negative yaw steering, while excess *decay* rates prevail during periods of positive yaw steering. Also apparent arc abrupt changes in the excess boost/decay levels upon entering and exiting periods of fixed yaw and after a yaw flip. These variations arc consistent with a combination of satellite body-fixed forces and the forces arising from offsetting the SA pitch angle by B.

While this evaluation technique helped establish the presence of anomalous forces, it incorrectly assumes the forces are always proportional to the satellite drag acceleration. Instead, a separate estimate of an along-track force acting in the presence of nominal drag is needed to isolate the anomalous force. Before presenting these results, wc will first identify potential sources of the anomalous force and provide some physical interpretations.

SOURCES OF OBSERVED ANOMALOUS FORCES

IN'I'RODIJCI1ON

"1'here have been extensive efforts to model the forces acting on the satellite. The Precision Orbit Determination Team (PODT) at GSFC has developed a *box and wing* model of the satellite[13,14] and later tuned it using laser ranging data and dual-frequency Doppler measurements from the French DORIS tracking system.[15] This modeling effort will be continually refined.

In some cases, the force models in the Navigation Team (NAVT) software are considerably simpler than their PODT counterparts in order to minimize the computational burden while providing nccdcd accuracy for predicting the long-term ground track behavior. Drag and sunline forces arc based on the VMA,[6] **while** the gravity field is a **20x20** truncation of the GEMT3 model' The PODT requires a much larger degree and order model (up to 70x70). The NAVT models were entirely adequate to the task *until* the decision to offset the SA by angle B was made shortly before launch.

Several potential sources of the anomalous forces were identified:

1) Outgassing from the interior of the satellite. These body-fixed forces arc expected to be constant in direction and to decline with time as volatiles *bake out.* Thus all body-fixed components should decay simultaneously. Outgassing is believed to be the primary source of the early *large* orbital decay forces.

2) Curling of the solar array duc to temperature differences between front and back produces a force in the satellite +Y-direction. This force is primarily dependent on reflected sunlight and is proportional to the curl angle.

3) 'f'here is a net thermal force duc to radiation from the satellite surfaces. Such forces are treated as body-fixed, but can vary with sun angle and yaw mode.

4) Unmodeled (in the NAVT software) forces arising from reflections from the offset solar array. The PODT carefully models these forces.

---

* The NAVT used a 20x2,0 truncation of GEMT3 from launch until 27 July 1993, when it was replaced by a 20x20 truncation of JGM2 at the same time the SA pitch offset angle B was reduced from 57.S to 53 deg.

Other sources considered but not discussed here include outgassing from the satellite blankets (after heating) and the (unmodeled) high-gain antenna used to communicate through the TDRSS. The possibility of leaky thrusters was quickly rejected in favor of an outgassing mode] for the early large declining force.

Our analysis is presented in two parts. The first part demonstrates the effect of body-fixed forces in the different yaw modes. The second part estimates the effect of the unmodeled reflections from the solar array in the different yaw modes. By such analytic modeling the effect of changing sun angle, solar array offset, and other factors can be predicted and serve to verify and help interpret inflight observations.

EFFECTS OF SATELLITE BODY-FIXED FORCES

Both pre-launch studies[6] and perturbation analyses have shown that only forces along the velocity vector are important in the long-term behavior of the ground track. Secular perturbations in eccentricity and argument of periapse can arise from once-per-orbit forces, both radial and along track, but these effects need not be considered here.

Shapiro[16] was the first to analyze the effects of constant (over an orbit) body-fixed forces in the various yaw modes. Figure 3 summarizes these results in terms of the rate of change in semi-major axis when the nominal yaw mode switch points are utilized (Eq. 1). The analysis shows that semi-major axis is affected by forces in the X-direction only in the two fixed-yaw modes; orbital boost occurs when flying forward, and orbital decay when flying backward. During yaw steering the net effect from the X-direction is zero. Similary, Y-direction forces are unimportant during the fixed yaw modes, but are important in the yaw steering modes. In positive yaw steering a +Y-axis force causes orbital decay at a rate that increases with β' angle. In negative yaw steering orbital boost of the same magnitude is expected. These distinctive signatures of X- and Y-body forces are helpful in interpreting the observed changes in semi-major axis.

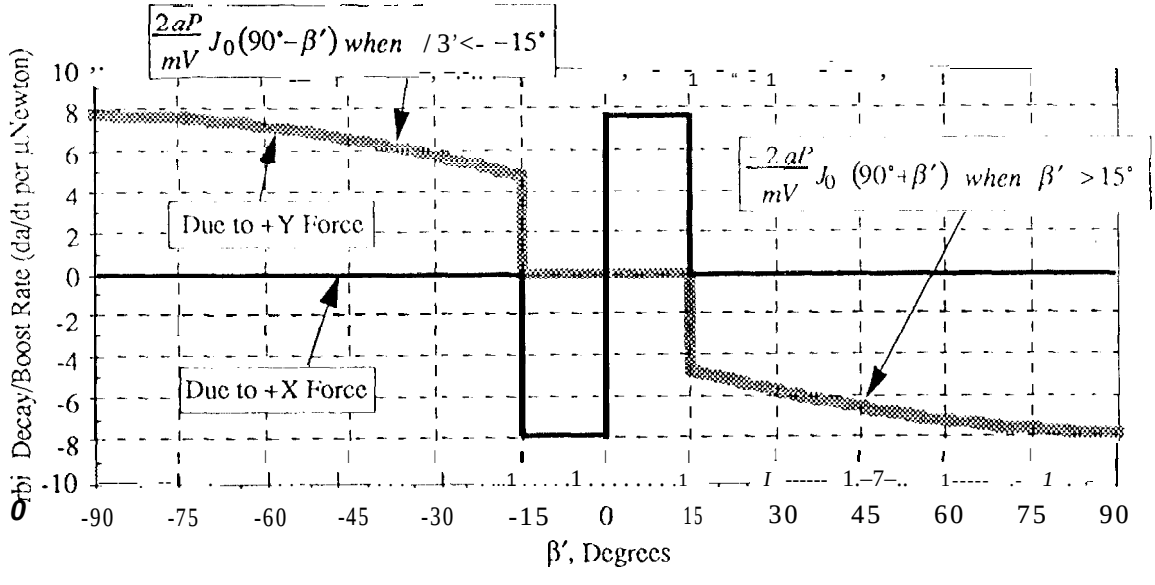

Figure 3 Daily Changes in da/dt (cm/day) vs β' for a Continuous Body-Fixed Thrust of 1μN (assumes nominal fixed yaw intervals: $-15° < \beta' < 15°$)

UNMODELED FORCES ARISING FROM THE SOLAR ARRAY OFFSET

The SA offset angle B (Eq. 3) is expected to be adjusted annually to compensate for performance degradation. A perturbation analysis was used to isolate the effects of reflections from the offset SA, as these forces are not modeled in the navigation software. Earth albedo effects and lags in reaching thermal equilibrium were ignored.

The force normal to the solar array duc to specular and diffuse reflection was resolved into satellite body-fixed coordinates as a function of the solar orbit angle (S2) for the different yaw modes. The body-fixed coordinates were then mapped into an earth-centered rotating coordinate system. An orbital average of the forces along the satellite velocity vector and their Fourier coefficients were then determined.

During yaw steering the average acceleration along the velocity is zero even during periods having solar occultation. During the fixed-yaw modes the average acceleration b_0 is

$$b_o = a_N \sin B \left[\frac{\sin(\Omega_{occ}/2)}{\pi} \right] \tag{5}$$

for the *fly-forward* mode, where a_N is the magnitude of the acceleration duc to the reflections from the solar array and Ω_{occ} is the angular length of the occultation interval. In the *fly-backward* mode the acceleration is in the opposite direction. If the SA offset is changed from lead to lag the force also reverses. During all fixed-yaw periods (except the first two when $\psi_s = -0^\circ$) a solar array *lead* angle was used. '1'bus, this force reverses at the yaw-flip (except for the two cases noted). The acceleration a_N is

$$a_N = \frac{2 G_S A_{sa}}{mc} \eta^* \cos^2 B \cos^2 \beta' \tag{6}$$

where G_S is the direct solar flux in W/m^2, A_{sa} is the solar array area, η^* is a composite array reflectivity, and c is the speed of light. Combining Eqs. 5 and 6 and expressing Ω_{occ} in terms of β'.

$$b_0 = \frac{2 G_S A_{sa}}{mc} \eta^* \left(\sin B \cos^2 B \right) \left(\frac{\cos^2 \beta'}{\pi} \sqrt{1 - (\cos\lambda / \cos\beta')^2} \right), \quad |\beta'| < \lambda \tag{7}$$

where $\lambda = 55.7,^0$ the value of β' when the occultation duration is zero. The maximum value of b_0 occurs when $B = 35.3$. " The decrease in b_0 *is* -8% at $\beta' = 15$", and ~31% at 30". 'typically, b_0 is -1.26 nm/s^2 when $\beta' = 0^\circ$ for B = 57.5," providing a boost in the mean semi-major axis of -23 cm/day. Eq. (7) describes the fly-forward mode; the acceleration reverses for the fly-backward mode.

Corroboration of these analytical results has been provided by Richter's thermal analysis[17] which reproduces observed solar array temperature quite well over the full range of β' angles.

ESTIMATING THE ANOMALOUS FORCE

By 21 Scp 92 the maneuver sequence designed to acquire operational orbit conditions had been successfully completed.[4] Each of the six maneuvers repeatedly interrupted newly-stable orbit conditions, precluding opportunities to confidently establish a trend in the anomalous along-track force. Fortunately, this limitation had been acceptable, since orbit changes induced by these maneuvers were much greater than the effects of the observed decay phenomena. However, once

operational orbit conditions had been achieved, effective ground track maintenance then depended on reliable estimates of the anomalous forces, since the related orbital decay and boost rates were generally the same order-of-magnimdc as the expected decay due to atmospheric drag.

Plans were made to estimate an along-track thrust multiplier (1-I τ) as part of routine orbit determination. Only τ would be estimated, and not the drag multiplier (1+-PI) since these along-track forces could not be satisfactorily estimated simultaneously. Brief studies quickly established that a single τ acting over a tracking arc of at least five days was necessary for confident estimation. Shorter tracking arcs, or more frequent (daily) τ estimates, were poorly determined and unsuitable for trend analysis.?

A strategy was adopted to estimate a single τ acting over a seven-day tracking arc, This technique would establish an average thrust force referred to the center of the tracking data arc. A daily moving average τ was obtained by advancing the seven-day tracking arc by a day and dropping off the first day, so adjacent solutions were always based on six days of common tracking data. This method produces a reasonably smooth and consistent daily history of τ which can then expressed as an equivalent rate of change in orbit mean semi-major axis, &z/dr,'8

$$T_{LT} = (1+\tau), \text{ in } \mu\text{N}$$

$$\text{then } \frac{da}{dt} = \frac{P}{\pi}\left(\frac{T_{LT}}{m}\right) \cong 7.7 T_{LT} \quad \left(\frac{da}{dt} \text{ is in cm / day when } T_{LT} \text{ is in } \mu\text{N}\right) \tag{8}$$

where T_{LT} is the along-track thrust, τ is the estimated thrust parameter, J' is the orbit period, and m is the satellite mass.

Finally, orbit determination solutions were isolated into distinct families corresponding to each of the four yaw control modes. This grouping technique was essential to prevent corruption of an orbit solution with dramatically different force levels known to be present in adjacent yaw control modes (e.g., Figure 3). Ultimately, the desired prediction model should cover a period of at least three or four months, the approximate spacing between orbit maintenance maneuvers. Such a model would define the behavior of the anomalous force during each of the four yaw control modes, as each mode would bc used at least once between orbit maintenance maneuvers.

The anomalous forces arc first examined during periods of negative and positive yaw steering, then for fixed yaw, flying both forward and backward. Finally, these individual segments arc assembled to form a composite prediction model for USC. in orbit maintenance.

FORCES OBSERVED D URING NEGATIVE YAW STEERING

Stable orbit conditions suitable for estimating the anomalous force were first available socm after achieving the operational orbit. The satellite was in a period of negative yaw steering ($\beta' <$ O). Unfortunately, this initial opportunity was necesarily brief, since the first orbit maintenance maneuver (OMM1) had already been planned to reverse the eastward drift of the ground track and to begin the orbit maintenance phase. Recognizing that predictions of the anomalous force were now needed for effective OMM1 design, the Project permitted the ground track to drift beyond the eastern control boundary, scheduling OMM 1 on 13 Ott 92 at the transition between Cycles 2 and 3 (originally OMM1 would have occurred -10 days earlier between Cycles 1 and 2).**

* Early in the mission two 40-min passes/orbit of two-way Doppler via TDRS East and West were used; in May 1993 tracking was reduced to onc 40-min pass/orbit of one-way Doppler.

** See the ground track history shown later in Figure 12.

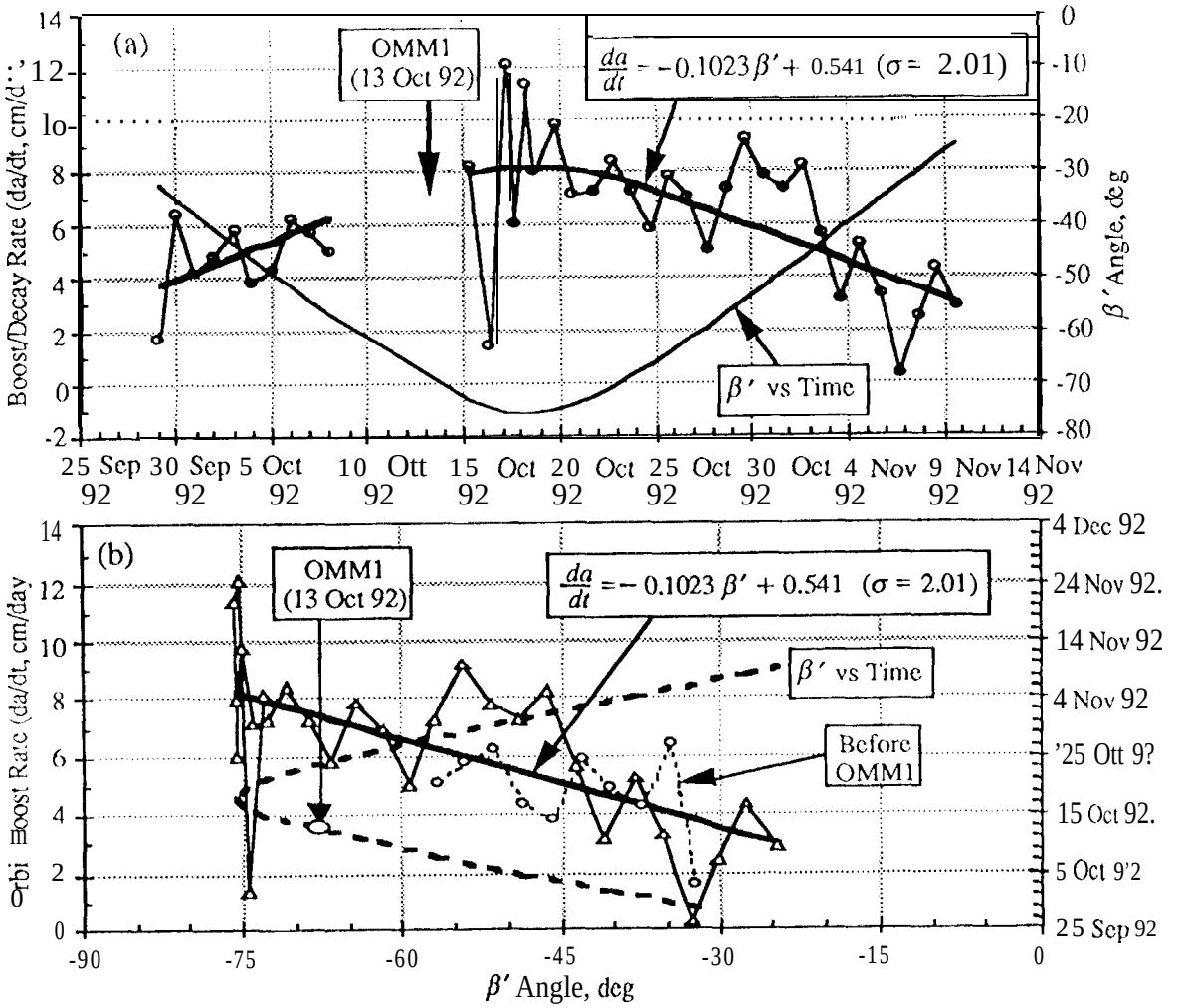

Figure 4(a) **Estimate of Orbital Boost Due to Anomalous Force During Negative Yaw Steering (Time Dependence), and (b) β' Dependence**

This operational plan provided a limited Lhrcc-week period prior to OMM 1 to obtain initial estimates of the anomalous force and to develop a prediction model covering about four months. Figure 4(a) shows that a small orbital boost rate was observed prior to OMM1, but these data did little toward development of a meaningful post-maneuver prediction model. Quick review of Figure 2(a) during the period prior to OMM 1 suggests that outgassing might have been the only force present, and may bc ending a long period of exponential decay. Because results from the daily τ estimates were so inconclusive, a decision was rnadc to apply a continuation of the exponential trend for an additional 17 days after OMMI, believing this would account for the remaining outgassing and possibly mark the end of any anomalous forces. The modest consequences of this incorrect choice in relation to the overall effectiveness of subsequent ground track maintenance arc discussed later.

Continued τ estimation after OMM 1 (Figure 4a) shows sustained orbit boost rates between ~3 and ~8 cm/day that are negatively correlated with the β' variation. A least-squares fit of the daily *da/dt* values over the entire negative yaw steering period results in a linear variation with β', as shown by Eq. (6) and illustrated in Figure 4(b).

$$\frac{da}{dt} = -\,0.1023\beta' + 0.541 \quad \left(\frac{da}{dt} \text{ in cm/day when } \beta' \text{ in deg}\right) \tag{9}$$

FORCES OBSERVED DURING POSITIVE YAW STEERING

The anomalous force was first estimated during positive yaw steering in late Nov 92. This interval was briefly interrupted by OMM2 on 21 Dec 92. Daily τ estimates indicated sustained orbital decay (Figure 5a) which were negatively correlated with the β' variation, a trend similar to that previously observed during negative yaw steering. Figure 5(b) and Eq. (1 O) show the decay rate varies linearly with β'.

$$\frac{da}{dt} = -0.1023\beta' - 3.131 \quad (\beta' \text{ in deg}, da/dt \text{ in cm / day}) \qquad (10)$$

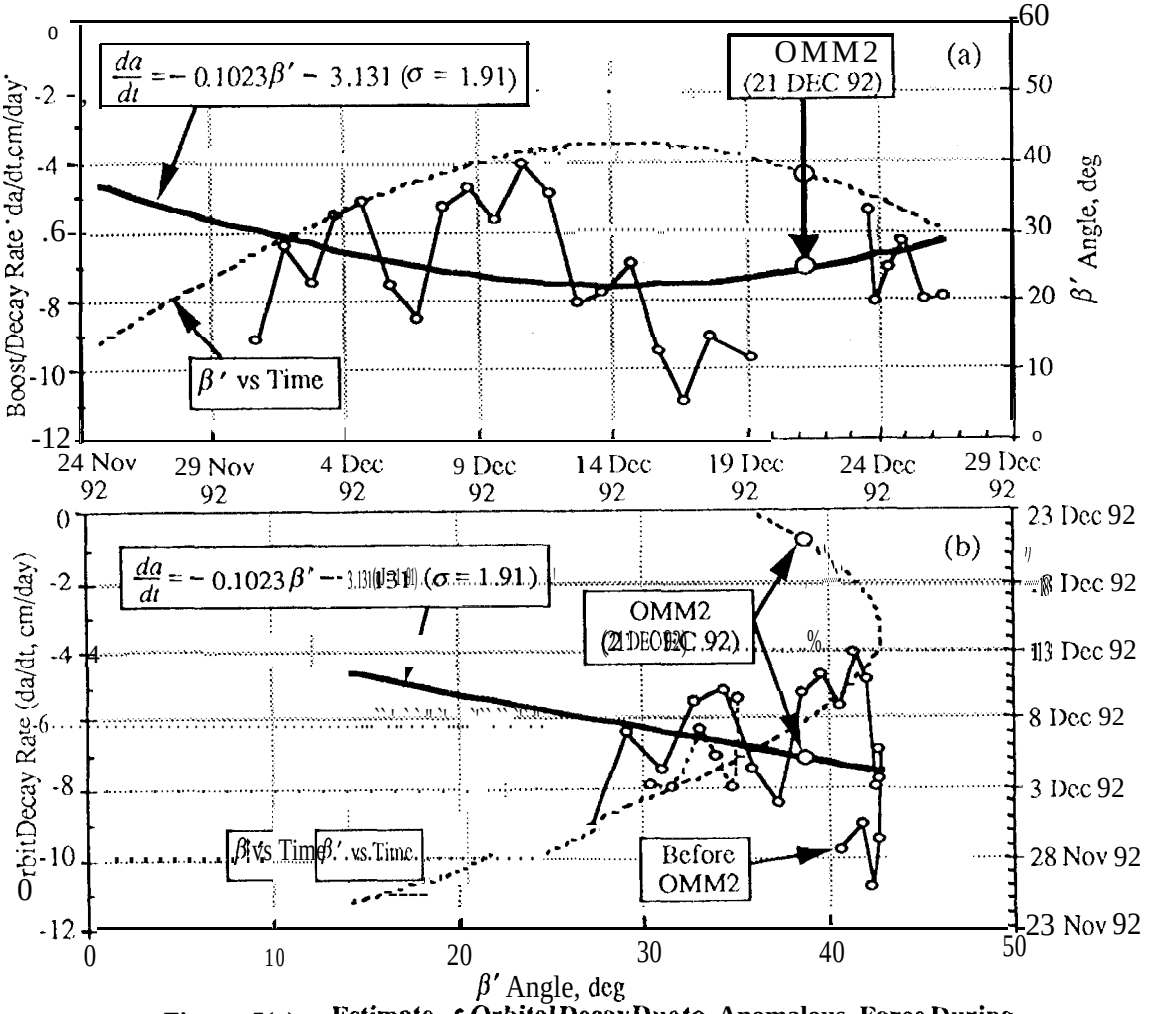

Figure 5(a) Estimate of Orbital Decay Due to Anomalous Force During Positive Yaw Steering (Time Dependence), and (b) β' Dependence

While the trends in the anomalous force with β' were similar, the observed orbital decay levels are -3.7 cm/day greater than were predicted by variations with β' determined earlier during negative yaw steering. A comparison of Eqs. 9 and 10 clearly describes this difference (also see Appendix A). Marshall[15] confirms with precision orbit determination using satellite laser ranging that the + Y forces were persistently different in these negative and postitive β' regimes. Differences in orbit-sun geometry may explain these differences. The average along-track force due to SA curling should be smaller during occultations due to the reduced time in sunlight.

When $|\beta'|$ 255.7°, the sate.llitc orbit enters and remains in full sun as β' varies through its peak value. " The peak β' value in Oct 92 was -76°; the orbit was in full sun for -?.() days. However, in Dcc 92 during the winter solstice, the peak β' value reached only -42" and full sun conditions were never achieved. This geometry repeats during every winter and summer solstice, while all the other β' cycles always provide extended periods of full sun. Richter's results[17] also predict an increase in the -t Y force upon entering full sun.

EMPIRICAL MODELS FOR POSITIVE AND NEGATIVE YAW STEERING

The previous sections have described the technique for estimating the anomalous force during positive and negative yaw steering modes, using two early sample periods. Figures 4 and 5, and Eels. 9 and 10, summarize these results. Through June 93, there have been a total of five different periods of yaw steering, three in the negative and two in the positive yaw steering mode.

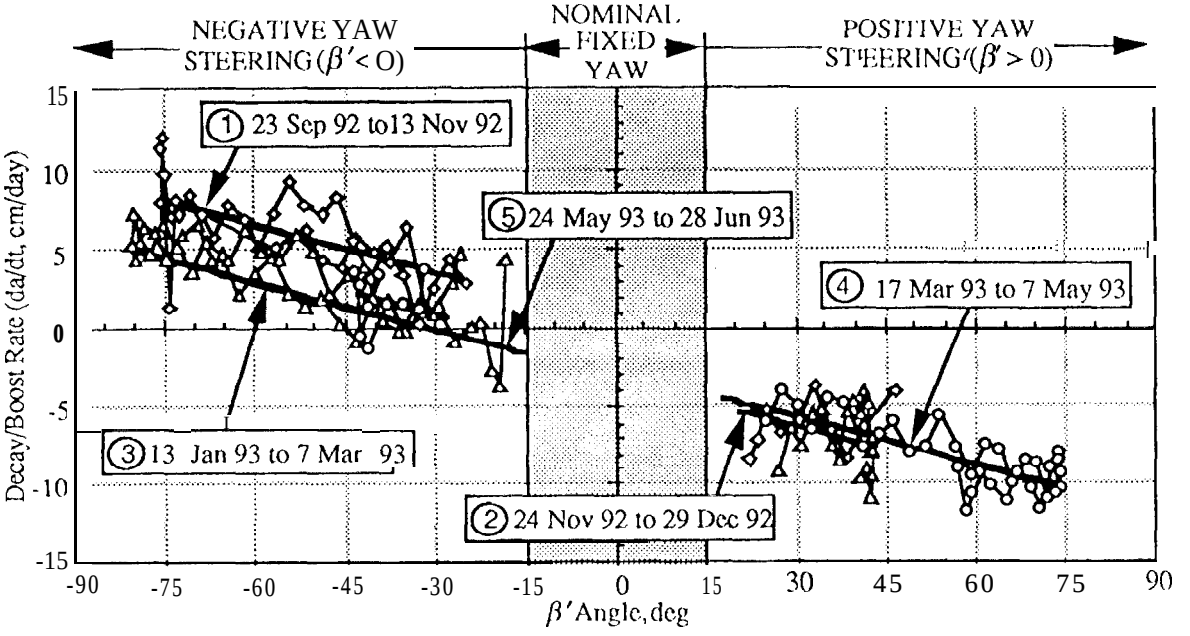

Figure 6 Composite Estimate of Orbital Decay/Boost Due to Anomalous Force for Both Positive and Negative Yaw Steering (β′ Dependence)

Figure **6 shows** the respective orbital boost or decay rates with β' for each of the five yaw steering periods. Periods 1, 3, and 5 arc consecutive repeats of the negative yaw steering mode when an orbital boost was observed. The boost rates estimated for period 1 arc -3.7 cm/day higher than those for period 3, whereas period 3 is -0.3 cm/day higher than period 5. The large reduction in boost rates between periods 1 and 3 may indicate additional decay due to residual outgassing, as the observed change is much larger than could be explained by errors in estimating τ. Also, periods 1 and 3 arc intervals of full sun, making direct comparisons more valid, Period 5 occurs near the 1993 summer solstice, and so it is reasonable to expect it to differ somewhat from the trend observed during period 3.

The two intervals of positive yaw steering shown in Figure *6*, periods 2 and 4, result in orbital decay. The empirical models for these two intervals indicate that period 4 has -0.5 cm/day less decay than period 2, a trend which supports the presence of additional outgassing. However, period 4 includes an interval of full sun, while period ? dots not, so direct comparison of these two periods may be less valid.

* See the β' history since launch later in Fig. 11.

Overall, the four most recent yaw steering periods have exhibited excellent repeatability, certainly well within the estimation accuracy of the empirical models (see Appendix A). The remaining task prior to establishing an overall prediction model suitable for use in orbit maintenance maneuver design requires estimates of the anomalous force during periods of fixed yaw.

FORCES OBSERVED DURING FIXED YAW

Periods of fixed yaw nominally occur when -15°< /3'< 15'. Five have occurred since launch. As indicated in Eq. (1) there are two fixed yaw control modes: flying forward when O"< β' < 15', and flying backward when $-15° < \beta' < 0°$. These modes are always separated by a yaw flip maneuver near $\beta' = O"$.

A trend model of the anomalous force for the two fixed-yaw modes was also developed by estimating a single thrust parameter τ over the tracking data arc. * 'l'he tracking data were carefully limited to the period of fixed yaw 10 avoid corruption of τ by data from adjacent yaw control modes where the along-track forces are dramatically different. A single fixed yaw mode covers about five days when nominal switch points are utilized. Since confident recovery of τ requires at least five days of tracking data, these solutions were sometimes marginally adequate.

However, there were two periods of fixed yaw extending outside $-15° < \beta' < 15"$ to support special circumstances. These longer periods of fixed yaw provided additional tracking data to facilitate more confident recovery of τ, while also presenting unique opportunities to observe the anomalous force during fixed yaw at β' angles above the nominal 15-deg limit. The first such occurrence was between 29 Dec 92 and 8 Jan 93 (-10 days). During this holiday period the satellite was placed in fixed yaw early when $\beta' \approx +23.7"$ while flying forward, remaining in this mode until a yaw flip was performed near $\beta' = -0"$. Between 13 and 24 May 93 (-1 1.5 days) the satellite remained in fixed yaw (flying backward) longer, until /3' ≈ –26. 7", to increase orbital decay needed to keep the satellite ground track from drifting outside the western control boundary soon after executing OMM3 on 30 Mar 93.**

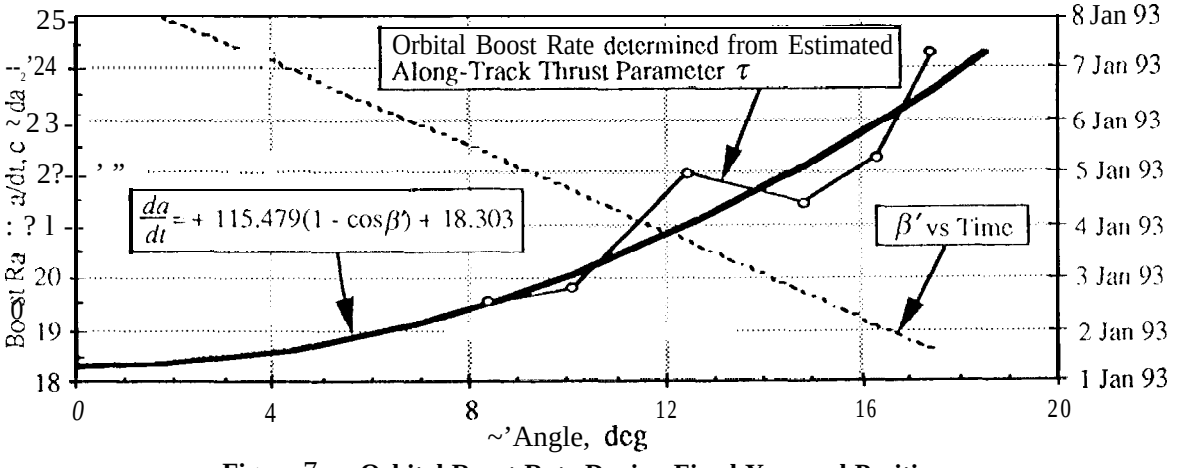

Figure 7 Orbital Roost Rate During Fixed Yaw and Positive β' (ψ_s = 0°) from 29 Dec 92 to 8 Jan 93 (-10 days)

* Tracking data aquisition during fixed yaw is the same as previously decribed for yaw steering (see p. 9).

** See the ground track history shown later in Figure 12.

Figure 7 shows an orbital boost that increases with β' during the period of fixed yaw between 29 Dec 92 and 8 Jan 93. The empirical model (Appendix A) describes this variation as a simple linear function of $(1 - \cos\beta')$. However, this result dots not support intuition that the along-track forces would decrease as /3' increases. Such a result would be expected as the solar incidence angle increases with /3', [hereby reducing the SA area projected normal to the along-track direction. In contrast, this surprising result was not duplicated in May 93 while flying backwards in fixed yaw. Figure 8 shows the +X forces reverse to cause orbit decay, steadily declining as β' increases, while varying linearl y with $(1 - \cos\beta')$, as also shown by the empirical model in Appendix A.

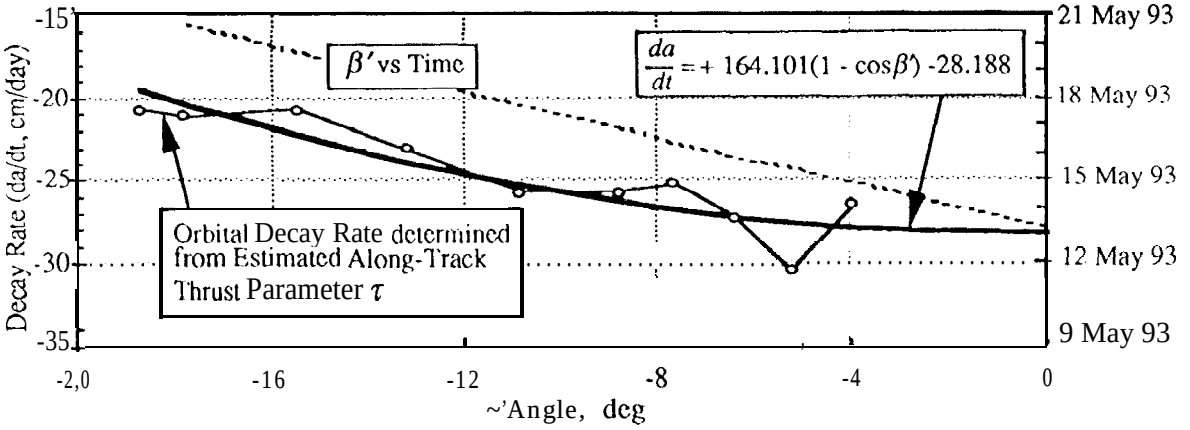

Figure 8 Orbital Decay Rate During Fixed Yaw and Negative β' (ψ_s = 180°) from 13 to 24 May 1993 (~11.5 days)

Before confronting the obvious conflict presented by these contradictory results, let us first compare them with *da/dt* estimates obtained during other periods of fixed yaw. Figure 9 combines the results of Figures 7 and 8 with estimates from other fixed yaw periods and these comparisons are quite good, but are necessarily limited to β' values near 7.5°, the average β' during nominal periods of fixed yaw covering about five days.

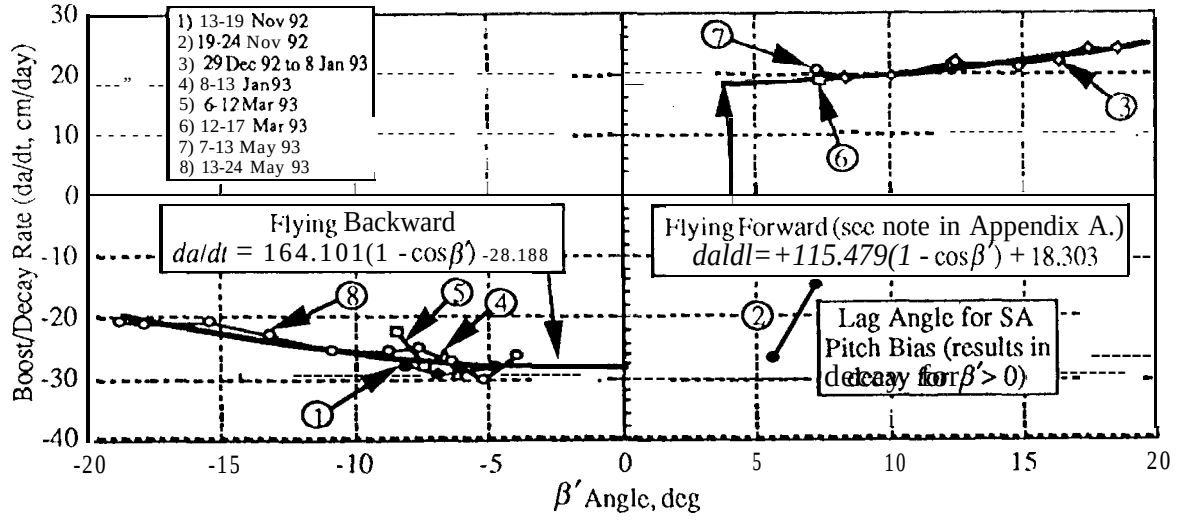

Figure 9 Orbital Boost/Decay Rates During Fixed Yaw for Positive and Negative β'

Richter's analysis[17] supports our analytical results (Eq. 7) that the orbital boost declines as β' increases. Also, quick-look orbit determination performed by the '1'OPEX/Poseidon Verification Team using laser ranging measurements confirm this trend. Ironically, the empirical function derived from τ estimates better describes the expected variation if the term + 115.479(1 - cos β') shown in Figure 7 were replaced by its negative: --1 15.479(1 – cos β'), as is shown in Appendix A. Usc of this more plausible model is planned for predicting future variations in da/dt with β' while flying forward in fixed yaw beyond $\beta' = -15°$. Additional experience in this control mode will help establish the appropriate empirical model.

COMPOSITE EMPIRICAL MODEL

Observations of the anomalous force during each yaw control mode have been used to develop empirical models of the rate of change in the mean semi-major axis (da/dt) as a function of the sun-orbit plane separation angle /3', These results were derived from daily estimates of an average along-track thrust parameter τ obtained from moving seven-day tracking arcs. Appendix A summarizes the resulting empirical models, identifying the time interval and β' values for each yaw mode.

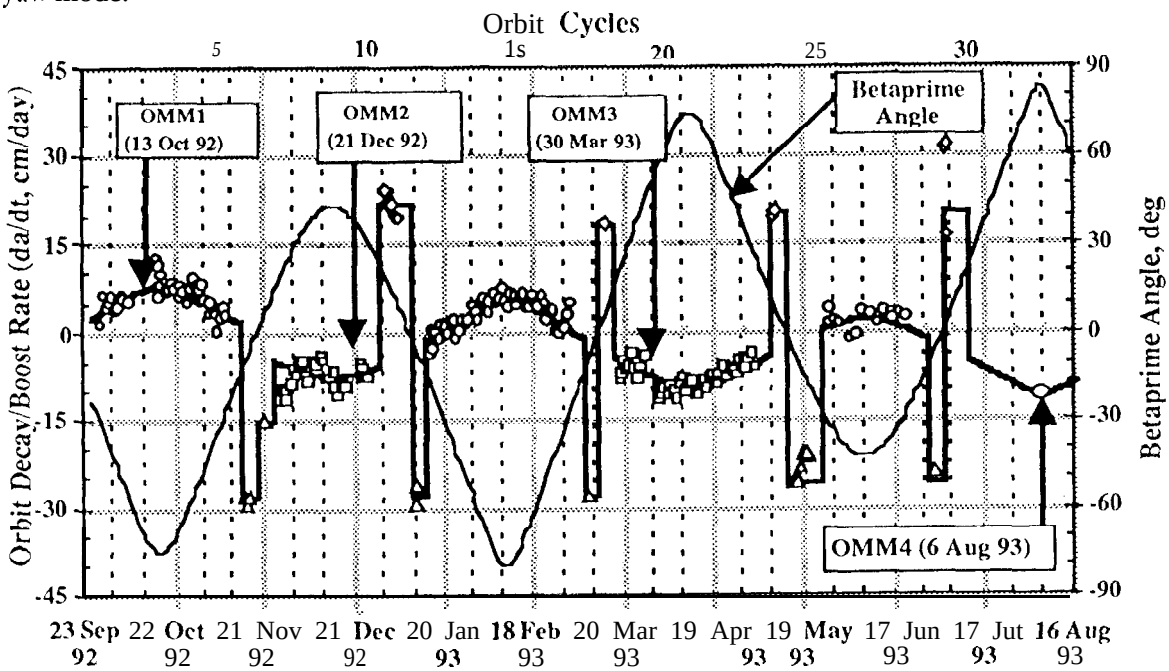

Figure 10 History and Prediction of Orbit Decay/Boost due to Anomalous Force

A composite of the empirical models is shown in Figure 10 for the period between late September 9210 mid-August 93.* This figure also shows the daily estimates of da/dt and locates each orbit maintenance maneuvers performed since launch. The variation of β' identities changes in yaw control mode. The *sawtooth* shape occurs when a yaw flip is performed ($\beta' = 00$), orbital boost results when $\beta' < 0°$ and orbital decay occurs when $\beta' > O$"

These results arc consistent with a force acting along the body +Y axis during yaw steering, (Figure 3) These forces appear to result from curling of the SA induced by a thermal gradient between the front and rear surfaces (Richter[17]). During fixed yaw the orbital boosts arc generally consistent with the predicted effects of the SA pitch pitch offset angle B summarized by Eq. (7).

* The discontinuity in the empirical model between orbit cycles 31 and 32 reflects the expected change due to reducing the SA pitch offset angle B from 57.5 to 53 deg.

EFFECTS ON THE SATELLITE GROUND TRACK

Prior to launch, drag was believed to be the most significant perturbation affecting the satellite ground track. Luni-solar gravity has predictable and significant periodic effects on the ground track comparable to those of drag,[6] and is routinely modeled as part of ground track maintenance. The relative effects of errors in predicting the anomalous forces and atmospheric drag are shown in Figure 11. Observed prediction errors are defined for the intervals between each orbit maintenance maneuver (Figure 11a). A comparison of these three curves shows modeling improvements since the anomalous force was initially observed.

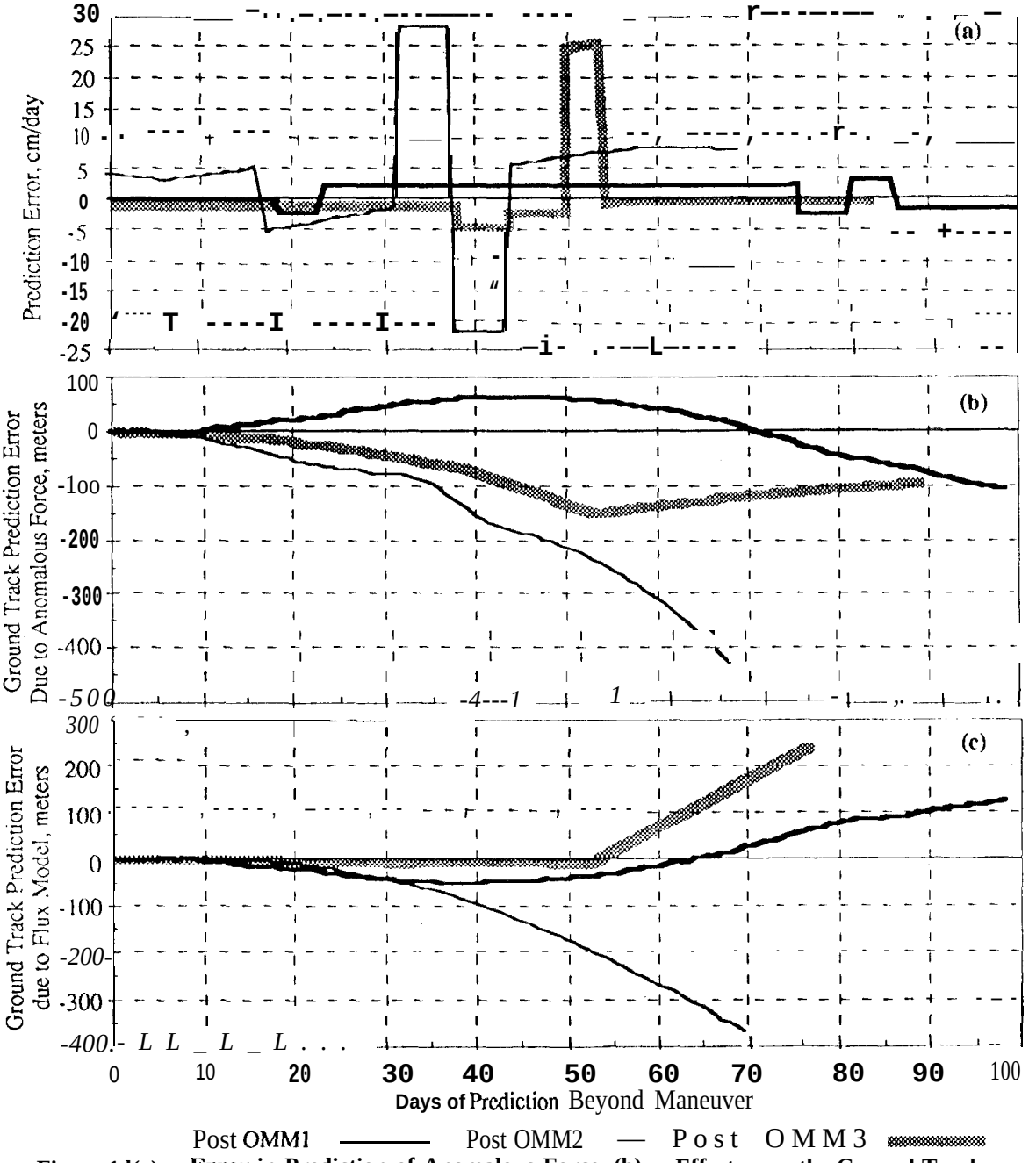

Figure 11(a) Error in Prediction of Anomalous Force, (b) Effect upon the Ground Track, and (c) Error in Ground Track Prediction due to Errors in the Flux Prediction Algorithm.

9 ’

The translation of these prediction errors into ground track units is shown in Figure 11(b), and the corresponding ground track errors due to solar flux prediction errors arc shown in Figure 11(c). These ground track errors were generated utilizing an analytic mean element propagation program (GTARG) which models all perturbations known to cause significant variations in the satellite ground track.[12] These perturbations include earth oblateness (zonals to J_{20}), luni-solar gravity, atmospheric drag, and the anomalous force. Drag predictions were obtained by repeating the NOAA/SESC 27-day outlook[20] as required to cover the prediction interval.[7] The ground track plots of Figure 11 were generated by differencing GTARG runs, but varying the boost (Figure 1 lb) and drag (Figure 1 1c) forces.

Physically, wc expect that an increase in the semi-major axis (from boost) will cause the ground track to accelerate westward, while a decrease moves the ground track eastward. Examination of Figure 11 confirms this physical intuition. If either the anomalous force or drag causes a smaller than expected decay, or the anomalous force causes a larger than expected boost, the true ground track falls west of the predicted ground track. These variations lead to the positive errors shown in Figure 11. Similarly, if the decay duc to drag is more than expected, or the boost from the anomalous force is less than expected, the true ground track falls cast of the prediction and this results in negative errors. For example, models available at the time of OMM 1 overestimated the initial predicted boost and ignored it altogether after 17 days. Initial overestimating led to an increasingly negative ground track error; mismodeling after 17 days and omitting the large effects of the fixed-yaw periods led to large errors in the expected directions.

Significant modeling improvements were realized by the time of the 0MM2 design. Slightly less than the expected decay was observed initially and during the first fixed yaw period, leading to a positive ground track prediction error. For approximately the next SO days, the net boost during yaw steering was overestimated, causing the ground track error to move continuously less westward and eventually turn eastward. These observations and the increased predictability of the anomalous force led the proposal to utilize the anomalous force for ground track maintenance by adjusting the duration of the fixed yaw periods. This strategy was used during the first fixed yaw period following 0MM3, as the ground track approached the western boundary, thereby obviating the need for an additional orbit maintenance maneuver.[21] As shown by Figure 12, our improved modeling has led to an increasing duration between maneuvers.

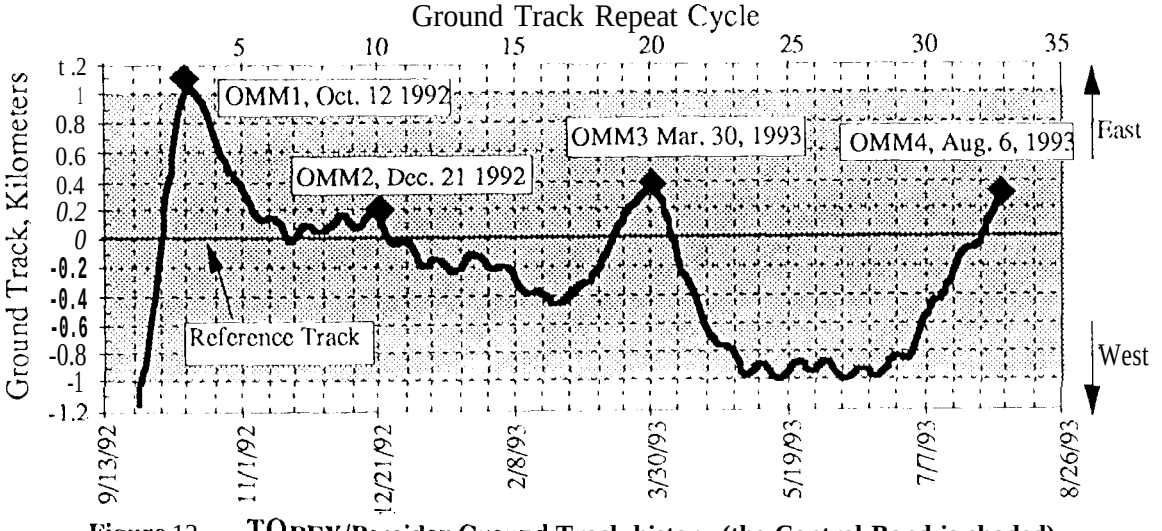

Figure 12 TOPEX/Poseidon Ground Track history (the Control Band is shaded).

SUMMARY

This paper describes the process by which the NAVT and the GSFC/FDF first detected, then began estimating, and finally developed an effective empirical model of the anomalous forces. The primary purpose of this task was to develop a prediction model for usc in ground

track maintenance. 'l'his objective has been realized by achieving increasingly longer times between orbit maintenance maneuvers. The spacing between OMM 1 and 0MM2 was 70 days, 100 days between OMM2 and OMM3, and 130 days between OMM3 and OMM4 (Figure 12).

Reasonable physical interpretations of the forces have also been identified, although further refinements arc expected and will be sought. Future work may include modeling of the changing SA curl effects with β' during yaw steering, particularly during full sun. Expected modeling changes imposed by adjusting the SA pitch bias arc better understood and now must be verified by flight data.

AC KNOWLEDGEMENTS

The authors and the NAVT wish to thank our PODT colleagues at GSFC and the University of Texas at Austin, and the Verification Team at JPL for sharing their results, thereby helping us to confirm ours. Notable thanks arc extended to John Ries at U of T, Andy Marshall at GSFC, and Chesley McColl at JPL. Wc also thank Bob Richter for sharing the initial results of his thermal anal ysis of the solar array.

Last, but certainly not least, wc owe great thanks and appreciation to the many GSFC/FDF personnel, and Ed Doll in particular, for their very professional and timely operational orbit determination support

REFERENCES

1. Tapley, B. D., "Orbit Determination Requirements for TOPEX," *AAS/AIAA Astrodynamics Specialist Conference,* August **1987,** Kalispell, Montana, AAS 87-429.

2. *"Ocean Topography Experiment (TOPEX)/Poseidon Flight Dynamics Facility (FDF)/TOPEX Project Interface Control Document,"* NASA/GSFC 553-FDD-92/029ROUD0, August 1992.

3. Bhat, R. S., "TOPEX/Poseidon Orbit Acquisition Maneuver Design," *AAS/AIAA Astrodynamics Specialist Conference,* Durango, Co., August 1991, AAS 91-514.

4. Bhat, R. S., Shapiro, B. E., Frauenholz, R. B., "TOPEX/Poseidon Operational Orbit Acquisition," *AAS/AIAA Astrodynamics Specialist Conference,* Victoria, B. C., Canada, August 1993, AAS 93-571.

5. Perrygo, C., *TOPEX Satellite Yaw Maneuvers,* Fairchild IOC REF: 968: SE:87-074, 11 November 1987.

6. Bhat, R. S., Frauenholz, R, B., Cannell, P. E., "TOPEX/Poseidon Orbit Maintenance Maneuver Design," *AAS/AIAA Astrodynamics Specialist Conference,* Stowe, Vi., August 1989, AAS 89-408.

7. Frauenholz, R. 13., Shapiro, B. E., "The Role of Predicted Solar Activity in TOPEX/Poseidon Orbit Maintenance Maneuver Design,' *AA S/AIAA Astrodynamics Specialist Conference,* Durango, Co., August 1991, AAS 91-515.

8. Jacchia, L. G., *Static Diffustion Models of the Upper Atmosphere with Empirical Temperature Profiles*, Smithsonian Astrophysical Observatory Special Report 170, 30 December 1964.

9. Jacchia, L. G., *Atmospheric Models in the Region From 1 IO to 200 km, in CIRA-72: COSPAR international Reference Atmosphere 1972,* cd. The Committee for the COSPAR International Reference Atmosphere (CIRA) of COSPAR (Committee on Space Research) Working Group 4, Akademic-Verlag, Berline, 1972.

10. Hamilton, Carol, J., *Fairchild Space Company TOPEX Project Projected Area Model for Precision Orbit Determination, FSC Dec.* Bo.968:TLVM:89- *193,* 11December 1989.

11. Escobal, Pedro Ramon, *Methods of Orbit Determination, Ncw York:* Krieger, 1983.

12. Sterne, T.E., *An Introduction to Celestial Mechanics,* New York: Interscience, 1960.

13. Marshall, J. A., et. al. *Modeling Radiation Forces Acting on TOPEX/Poseidon for Precision Orbit Determination,* June 1992.

14. Luthcke, S. B. and Marshall, J. A., *Non-conservative Force Model Parameter Estimation Strategy for TOPEX/Poseidon Precision Orbit Determination,* NASA TM104575, November 1992.

15. Marshall, J. Andrew, Luthcke, Scott B., *Non-Conservative Force Model Performance for Topex/Poseidon Precision Orbit Determination,* AAS/GSFC international Symposium on Space Flight Dynamics, April 1993, AAS93-268.

16. Shapiro, B. E., *Analysis of Expected AV from a Thruster Leak on the TOPEX Satellite,* JPL 10M 314.5-1657, 16 September 1992 (Internal Document).

17. Richter, Robert, *Radiation Forces Acting on the TOPEX/Poseidon Spacecraft Along the Velocity Vector due to the Solar Array - Initial Results,* JPL IOM 3544 -TOP-93-004, 8 July 1993 (Internal Document).

18. McCuskey, S. W, *Introduction to Celestial Mechanics,* Addison-Wesley Publishing Co., 1963.

19. Shapiro, B. E., Bhat, R. S., "GTARG-The TOPEX/Poseidon Ground Track Maintenance Maneuver Targeting Program," *AIAA Aerospace Design Conference,* Irvine, Ca., February 1993, AIAA 93-1129.

20. Nelson, I. Gayle, Gehred, Paul A., Hinnan, Joseph W., Hcckman, Gary R., "Users Guide to the *Preliminary Report and Forecast of Solar Geophysical Data,* November 1992, " *Preliminary Report and Forecast of Solar Geophysical Data,* U.S. Department of Commerce National Oceanic and Atmospheric Adminsitration Space Environment Services Center, SESC PRF 897, 10 November 1992.

21. Bhat, Ram and Shapiro, Bruce. *Use of the Anomalous Force In TOPEX/Poseidon Ground Track Maintenance;* Jet 'Propulsion Laboratory Interoffice Memorandum FOS 93-024, June 15, 1993 (Internal Document).

Appendix A.
Empirical Models for the Anomalous Force vs Yaw Control Mode

YAW CONTROL MODE	START m	END (UTC)	EMPIRICAL MODEL (da/dt, cm/day, deg)	σ cm/d
Yaw Steering, $\beta' < 0$	23 Sep 92, 22:24:54	13 Nov 92, 08:00:08	$-0.1023\beta' + 0.541$	2.01
Fixed Yaw($\psi_s = 180°$) $-14.8° < \beta' < 0.2°$	13 Nov 92, 08:28:18	19 Nov 92, 01:45:57	−28.41	0.65
Fixed Yaw($\psi_s = 0°$) $+0.2° < \beta' < +14.1°$	19 Nov 92, 02:42:11	24 Nov 92, 18:08:05	−14.93	1.5
Yaw Steering, $\beta' > 0$	24 Nov 92, 18:36:12	29 Dec 92, 18:38:03	$-0.1023\beta' - 3.131$	1.91
Fixed Yaw($\psi_s = 0°$) $+23.6° < \beta' < -0.3°$	29 Dec 92, 19:06:10	8 Jan 93, 18:34:24	$-115.479(1 - \cos\beta') + 18.303$ (see footnote below)	0.70
Fixed Yaw($\psi_s = 180°$) $-0.3° < \beta' < -13.3°$	8 Jan 93, 19:30:22	13 Jan 93, 17:07:42	−27.53	2.26
Yaw Steering, $\beta' < 0$	13 Jan 93, 17:35:50	7 Mar 93, 00:12:30	$-0.1023\beta' - 2.228$	1.56
Fixed Yaw($\psi_s = 180°$) $-15° < \beta' < 0°$	7 Mar 93, 00:40:37	12 Mar 93, 02:57:59	−25.22	3.86
Fixed Yaw($\psi_s = 0°$) $0° < \beta' < 15°$	12 Mar 93, 03:54:00	17 Mar 93, 08:04:05	+18.6	1.48
Yaw Steering, $\beta' > 0$	17 Mar 93, 08:32:18	7 May 93, 12:51:02	$-0.1023\beta' - 2.560$	1.48
Fixed Yaw($\psi_s = 0°$) $+15° < \beta' < 0°$	7 May 93, 13:19:04	13 May 93, 07:33:12	+20.04	0.84
Fixed Yaw($\psi_s = 180°$) $0° < \beta' < -26.5°$	13 May 93, 08:29:10	24 May 93, 19:34:39	$164.101(1 - \cos\beta') - 28.188$	1.41
Yaw Steering, $\beta' < 0$	24 May 93, 20:03:04	28 Jun 93, 18:12:00	$-0.1023\beta' - 1.935$	1.84
Fixed Yaw($\psi_s = 180°$) $-13.1° < \beta' < 0°$	28 Jun 93, 18:40:00	4 Jul 93, 02:36:00	−23.97	1.48
Fixed Yaw($\psi_s = 0°$) $0° < \beta' < 15°$	4 Jul 93, 03:32:00	12 Jul 93, 03:11:00	+15.91	1.48

A least-squares fit of *da/dt* determined from equivalent estimates of τ resulted in the term $+115.479(1 - \cos\beta')$ (see Figure 7). which implies an increase in *da/dt* with β' when a decrease would be expected. Richter's analyses[17] and quick-look mbit determination by the JPL Verification Team using satellite laser ranging data confirm a decreasing trend. The term $-115.479(1 - \cos\beta')$ listed above better describes the expected variation with β' and will be used for predictions until additional flight data arc available to refine. the model.